

## Electronic Supplementary Information

### Hetero-bimetallic paddlewheel clusters in coordination polymers formed by a water-induced single-crystal-to-single-crystal transformation

Jorge Albalad,<sup>a</sup> Javier Ariñez-Soriano,<sup>a</sup> José Vidal-Gancedo,<sup>b</sup> Vega Lloveras,<sup>b</sup> Jordi Juanhuix,<sup>c</sup> Inhar Imaz,<sup>a\*</sup> Núria Aliaga-Alcalde<sup>bd</sup> and Daniel Maspoch<sup>\*ad</sup>

<sup>a</sup> Catalan Institute of Nanoscience and Nanotechnology (ICN2), CSIC and The Barcelona Institute of Science and Technology, Campus UAB, Bellaterra, Spain.

<sup>b</sup> Institut de Ciència de Materials de Barcelona (ICMAB-CSIC), Bellaterra, Spain and CIBER-BBN, Barcelona, Spain.

<sup>c</sup> ALBA Synchrotron, 08290 Cerdanyola del Vallès, Barcelona, Catalonia, Spain

<sup>d</sup> ICREA, Pg. Lluís Companys 23, 08010 Barcelona, Spain.

#### Contents:

---

#### S1. Experimental Section

##### S1.1. Materials and methods

##### S1.2. Synthetic procedure

Phase 1 [M(CuDOTA)·H<sub>2</sub>O] synthesis

Phase 2 [M(CuDOTA)·H<sub>2</sub>O]·4H<sub>2</sub>O synthesis

##### S1.3. Characterization

**Table S1.** Crystal and refinement data of **1**<sub>CuZn</sub> and **2**<sub>CuZn</sub>

**Table S2.** Metal proportion on bimetallic Phase 1 crystals measured by EDX analysis

**Table S3.** Metal proportion on bimetallic Phase 1 crystals measured by ICP-OES analysis

**Table S4.** Metal proportion on bimetallic Phase 2 crystals measured by EDX analysis

**Table S5.** Metal proportion on bimetallic Phase 2 crystals measured by ICP-OES analysis

**Table S6.** ICP-OES measurements of the transition water after 72 hours

**Figure S1.** XRPD diagrams of simulated and experimental CuH<sub>2</sub>DOTA.

**Figure S2.** XRPD diffractograms of the synthesized **1**<sub>CuZn</sub>, **1**<sub>CuCu</sub> and **1**<sub>CuNi</sub>, as compared to the simulated powder pattern for the crystal structure of **1**<sub>CuZn</sub>.

**Figure S3.** Crystal structure of **1**<sub>CuZn</sub>.

**Figure S4.** X-band EPR spectrum of Cu-DOTA, experimental (blue) and simulated (red).

**Figure S5.** X-band EPR spectrum of **1**<sub>CuZn</sub>, experimental (blue) and simulated (red)

**Figure S6.** Optical microscopy images showing the evolution of the water-triggered transition from **1**<sub>CuZn</sub> to **2**<sub>CuZn</sub>.

**Figure S7.** XRPD diffractograms of the synthesized **2**<sub>CuZn</sub>, **2**<sub>CuCu</sub> and **2**<sub>CuNi</sub>, as compared to the simulated powder pattern for the crystal structure of **2**<sub>CuZn</sub>.

**Figure S8.** Crystal structure of **2**<sub>CuZn</sub>.

**Figure S9.** XRPD diffractograms of the synthesized **2**<sub>CuZn</sub> after 6 months immersed in water and after 1 hour immersed in boiling water, as compared to the simulated powder pattern for the crystal structure of **2**<sub>CuZn</sub>.

**Figure S10.** Water adsorption isotherm of **1**<sub>CuZn</sub> and **2**<sub>CuZn</sub>.

**Figure S11.** XRPD diffractograms of the activated **2**<sub>CuZn</sub> (blue) and **2**<sub>CuZn</sub> after measuring the water isotherm, as compared to the simulated powder pattern for the crystal structure of **2**<sub>CuZn</sub>.

**Figure S12.** Experimental *c*<sub>M</sub>T vs T data of systems (a) **2**<sub>CuCu</sub> and (b) **2**<sub>CuZn</sub> (●) and fitting (red line) between 2.0 and 300.0 K using a dc external magnetic field of 1 T.

# S1. Experimental Section

## S1.1. Materials and Methods

All chemical reagents and solvents were purchased from commercial sources and used as received without further purification. Purity of all bulk materials was confirmed through X-Ray powder diffraction measurements (XRPD) collected on an X'Pert PRO MPD analytical diffractometer (Panalytical at 45 kV and 40mA using Cu K $\alpha$  radiation ( $\lambda= 1.5419 \text{ \AA}$ ) and compared with single crystal simulated patterns. Elemental Analyses were performed on a Flash EA 2000 CHNS (Thermo Fisher Scientific) analyser. Metal ratio on the final bulk materials were confirmed through ICP-OES using a Perkin Elmer Optima 4300DV instrument or through EDX measurements on a FEI Quanta 650F Environmental SEM. Gravimetric water sorption measurements were performed at 298 K using a flow of nitrogen, up to relative humidity (RH) of 95% with a DVS-Advantage-1 (Surface Measurements Systems Ltd.). The relative humidity inside the chamber was adjusted by bobbling a carrier gas (N<sub>2</sub>) in pure water until stream saturated in water (95% RH). The adsorbed moisture was expressed as  $g_{\text{water}}/g_{\text{dry sample}}$ . Prior to the water adsorption measurements, samples were outgassed each cycle at 120 °C during 3 hours using a heating rate of 0.5 °C/min. The EPR spectra were recorded on crystalline powder at 140 K in a Bruker ELEXYS E500 X-band spectrometer equipped with a TE102 microwave cavity, a Bruker variable temperature unit, and a field-frequency (F/F) lock system Bruker ER 033 M. Line positions were determined with an NMR Gaussmeter Bruker ER 035 M. The modulation amplitude was kept well below the line width, and the microwave power was well below saturation. Magnetic susceptibility measurements were performed on polycrystalline samples with a DMS5 Quantum Design susceptometer working in the range 1.8-300.0 K under a magnetic field of 0.1 T. TIP is the temperature-independent paramagnetism. Diamagnetic corrections were estimated from Pascal Tables.

## S1.2. Synthetic Procedure

### Synthesis of $1_{\text{CuZn}}$

In a screw capped vial,  $\text{CuCl}_2 \cdot 2\text{H}_2\text{O}$  (12.8 mg, 0.075 mmol) and  $\text{H}_4\text{DOTA}$  (30.3 mg, 0.075 mmol) were solved in 4 mL of distilled  $\text{H}_2\text{O}$  under sonication. After 5 minutes, a light-blue precipitate appeared corresponding to the discrete supramolecular complex  $\text{CuH}_2\text{DOTA} \cdot [\mathbf{1}] \cdot \text{Zn}(\text{NO}_3)_2 \cdot 6\text{H}_2\text{O}$  (43.9 mg, 0.15 mmol) solved in 4 mL of DMF was added afterwards. The resulting mixture was heated for 12 hours at  $120^\circ\text{C}$ , obtaining plated-shaped sky blue crystals (28.0 mg, 66% based on  $\text{H}_4\text{DOTA}$ ). Crystals were washed three times with 5 mL of DMF and maintained under the same solvent at room temperature. Found C 34.7 %, H 4.7 %, N 10.0 %.  $\text{CuZnC}_{16}\text{H}_{26}\text{N}_4\text{O}_9$  requires 35.1 %, H 4.8 %, N 10.2 %.

### Synthesis of $1_{\text{CuNi}}$

In a screw capped vial,  $\text{CuCl}_2 \cdot 2\text{H}_2\text{O}$  (12.8 mg, 0.075 mmol) and  $\text{H}_4\text{DOTA}$  (30.3 mg, 0.075 mmol) were solved in 4 mL of distilled  $\text{H}_2\text{O}$  under sonication. After 5 minutes,  $\text{Ni}(\text{NO}_3)_2 \cdot 6\text{H}_2\text{O}$  (40.5 mg, 0.15 mmol) solved in 4 mL of DMF was added afterwards. The resulting mixture was heated for 12 hours at  $120^\circ\text{C}$ , obtaining plated-shaped sky blue crystals (30.5 mg, 71% based on  $\text{H}_4\text{DOTA}$ ). Crystals were washed three times with 5 mL of DMF and maintained under the same solvent at room temperature. Found C 35.6 %, H 4.9 %, N 10.3 %.  $\text{CuNiC}_{16}\text{H}_{26}\text{N}_4\text{O}_9$  requires 35.6 %, H 4.9 %, N 10.4 %.

### Synthesis of $1_{\text{CuCu}}$

In a screw capped vial,  $\text{CuCl}_2 \cdot 2\text{H}_2\text{O}$  (12.8 mg, 0.075 mmol) and  $\text{H}_4\text{DOTA}$  (30.3 mg, 0.075 mmol) were solved in 4 mL of distilled  $\text{H}_2\text{O}$  under sonication. After 5 minutes,  $\text{Cu}(\text{NO}_3)_2 \cdot 2.5\text{H}_2\text{O}$  (35.7 mg, 0.15 mmol) solved in 4 mL of DMF was added afterwards. The resulting mixture was heated for 12 hours at  $120^\circ\text{C}$ , obtaining plated-shaped sky blue crystals (35.0 mg, 87% based on  $\text{H}_4\text{DOTA}$ ). Crystals were washed three times with 5 mL of DMF and maintained under the same solvent at room temperature.  $1_{\text{CuCu}}$  can also be synthesized by direct mixture of  $\text{H}_4\text{DOTA}$  and 2 equivalents of  $\text{CuCl}_2 \cdot 2\text{H}_2\text{O}$  in a water:DMF mixture and heating at the same temperature. Crystals were washed three times with 5 mL of DMF and maintained under the same solvent at room temperature. Found C 35.0 %, H 4.8 %, N 10.0 %.  $\text{Cu}_2\text{C}_{16}\text{H}_{26}\text{N}_4\text{O}_9$  requires 35.2 %, H 4.8 %, N 10.2 %.

### **Synthesis of 2<sub>CuZn</sub>**

30 mg of dry crystals of **1<sub>CuZn</sub>** were immersed in 5 mL of distilled water and left undisturbed at room temperature. A change of colour in the crystalline material from sky blue to green was observed at the same time that the solution became blueish. The transition was completed after 72 hours, in which PXRD measurements confirmed phase purity. The material was then washed three times with 10 mL of distilled water, and kept under the same solvent (18 mg). Found C 31.4 %, H 5.2 %, N 9.0 %.  $\text{Cu}_{1.5}\text{Zn}_{0.5}\text{C}_{16}\text{H}_{26}\text{N}_4\text{O}_9 \cdot 4\text{H}_2\text{O}$  requires 31.0 %, H 5.5 %, N 9.0 %.

### **Synthesis of 2<sub>CuNi</sub>**

30 mg of dry crystals of **1<sub>CuNi</sub>** were immersed in 5 mL of distilled water left undisturbed at room temperature. A change of colour in the crystalline material from blue to green was observed at the same time that the solution became blueish. The transition was completed after 2 months, in which PXRD measurements confirmed phase purity. The material was then washed three times with 10 mL of distilled water, and kept under the same solvent (18 mg). Found C 31.9 %, H 5.9 %, N 9.2 %.  $\text{Cu}_{1.5}\text{Ni}_{0.5}\text{C}_{16}\text{H}_{26}\text{N}_4\text{O}_9 \cdot 4\text{H}_2\text{O}$  requires 31.4 %, H 5.6 %, N 9.1

### **Synthesis of 2<sub>CuCu</sub>**

30 mg of dry crystals of **1-Cu** were immersed in 5 mL of distilled water and left undisturbed at room temperature. A change of colour in the crystalline material from blue to green was observed at the same time that the solution became blueish. The transition was completed after 96 hours, in which PXRD measurements confirmed phase purity. The material was then washed three times with 10 mL of distilled water, and kept in the same solvent (22 mg). Found C 32.0 %, H 5.8 %, N 9.3 %.  $\text{Cu}_2\text{C}_{16}\text{H}_{26}\text{N}_4\text{O}_9 \cdot 4\text{H}_2\text{O}$  requires 31.1 %, H 5.6 %, N 9.1 %.

### S1.3. Characterization

**Table S1.** Crystal and refinement data of **1<sub>CuZn</sub>** and **2<sub>CuZn</sub>**

Compound Reference	<b>1<sub>CuZn</sub></b>	<b>2<sub>CuZn</sub></b>
Chemical Formula	CuZnC <sub>16</sub> H <sub>26</sub> N <sub>4</sub> O <sub>9</sub>	CuZnC <sub>16</sub> H <sub>26</sub> N <sub>4</sub> O <sub>9</sub> ·4H <sub>2</sub> O
Formula Mass	547.35	619.5
Crystal System	Monoclinic	Monoclinic
Space group	P2/n	P2 <sub>1</sub> /c
a/ Å	10.950(4)	11.560(5)
b/ Å	6.350(4)	16.830(5)
c/ Å	13.610(4)	12.920(5)
$\alpha$ / °	90	90
$\beta$ / °	92.58(12)	110.97(3)
$\gamma$ / °	90	90
Unit Cell Volume / Å <sup>3</sup>	972.2(8)	2347.2(16)
Temperature / K	100	293
Z	2	4
Reflexions Measured	14404	24123
Independent Reflections	1126	4144
Reflections ( $I > 2\sigma(I)$ )	1065	3593
R <sub>int</sub>	0.088	0.067
R <sub>1</sub> ( $I > 2\sigma(I)$ )	0.0413	0.0549
wR( $F^2$ ) ( $I > 2\sigma(I)$ )	0.1095	0.1583
R <sub>1</sub> (all data)	0.0428	0.0616
wR( $F^2$ ) (all data)	0.1103	0.1641

**Table S2.** Metal proportion on bimetallic Phase 1 crystals measured by EDX analysis.

<b>Material</b>	<b>Cu (At %)</b>	<b>M (At %)</b>
<b>1<sub>CuZn</sub></b>	51.90	48.10
<b>1<sub>CuNi</sub></b>	50.78	49.22

**Table S3.** Metal proportion on bimetallic Phase 1 crystals measured by ICP-OES analysis.

<b>Material</b>	<b>Cu (mg/L)</b>	<b>M (mg/L)</b>
<b>1<sub>CuZn</sub></b>	202	210
<b>1<sub>CuNi</sub></b>	251	234

**Table S4.** Metal proportion on bimetallic Phase 2 crystals measured by EDX analysis.

<b>Material</b>	<b>Cu (At %)</b>	<b>M (At %)</b>
<b>2<sub>CuZn</sub></b>	75.05	24.95
<b>2<sub>CuNi</sub></b>	74.36	25.64

**Table S5.** Metal proportion on bimetallic Phase 2 crystals measured by ICP-OES analysis.

<b>Material</b>	<b>Cu (mg/L)</b>	<b>M (mg/L)</b>
<b>2<sub>CuZn</sub></b>	555	187
<b>2<sub>CuNi</sub></b>	378	120

**Table S6.** ICP-OES measurements of the transition water after 72 hours.

<b>Initial Material</b>	<b>Exact mass (mg)</b>	<b>V H<sub>2</sub>O (mL)</b>	<b>Cu ICP-OES (mg/L)</b>	<b>Zn ICP-OES (mg/L)</b>	<b>Cu/Zn % loss</b>
<b>1<sub>CuZn</sub></b>	17.8 mg	5.0 mL	98	206	<b>26%/51%</b>

**Figure S1.** XRPD diagrams of simulated (black) and experimental (blue)  $\text{CuH}_2\text{DOTA}\cdot[\mathbf{1}]$

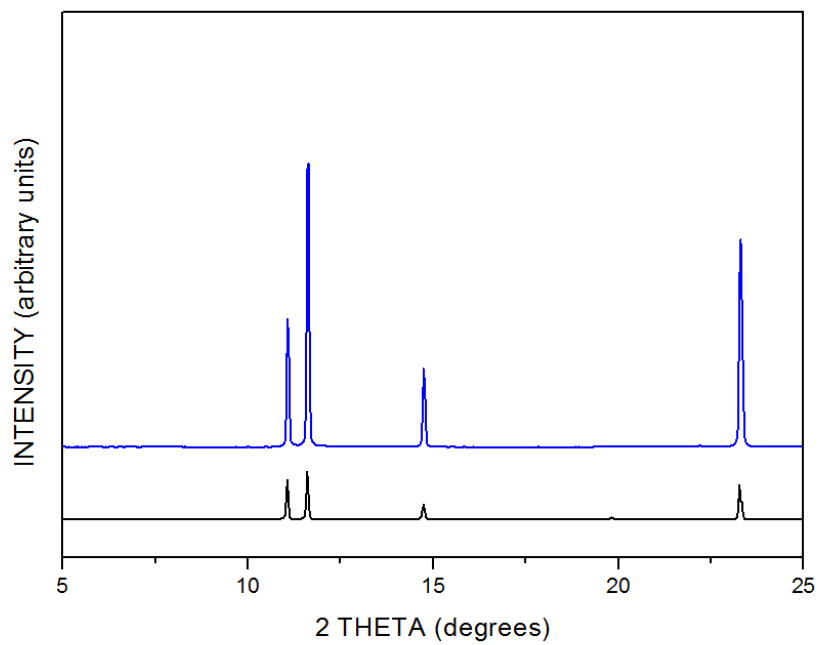


**Figure S2.** XRPD diffractograms of the synthesized  $\mathbf{1}_{\text{CuZn}}$  (purple),  $\mathbf{1}_{\text{CuCu}}$  (red) and  $\mathbf{1}_{\text{CuNi}}$  (blue), as compared to the simulated powder pattern for the crystal structure of  $\mathbf{1}_{\text{CuZn}}$  (black).

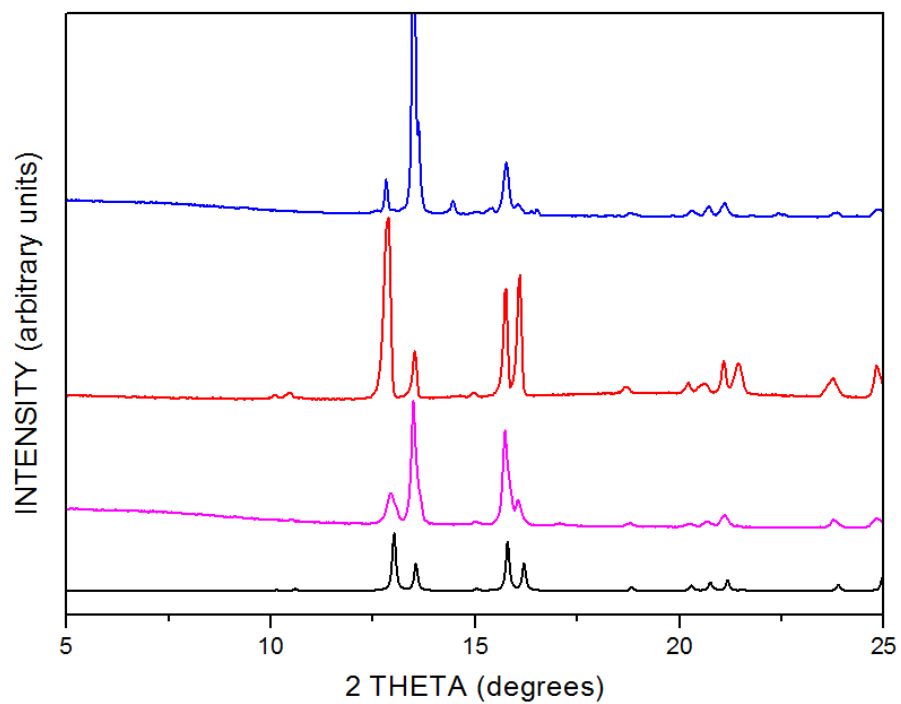
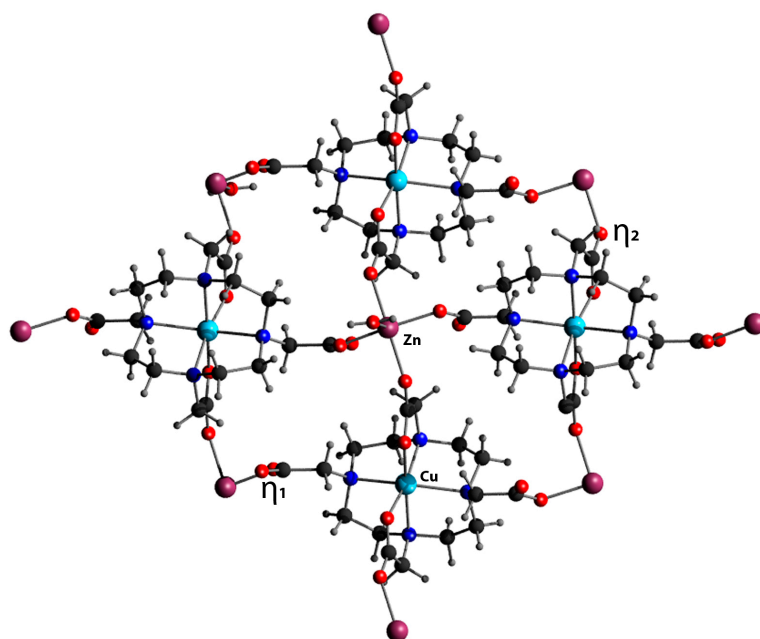


**Figure S3.** Crystal structure of **1<sub>CuZn</sub>**. (a) Coordination environment on the Cu-DOTA subunit and representation of the Zn(II) square-based pyramidal unit, with a view across the *a* crystallographic axis, showing both  $\eta_2$  and  $\eta_1$  acetate arms. (b) View of the hydrogen-bonded packing structure of **1<sub>CuZn</sub>**. Hydrogen bonds are marked as sky-blue dash lines. Atomic color code: Zn, plum; Cu, sky blue; C, black, O, red, N, blue; H, light grey.

a)



b)

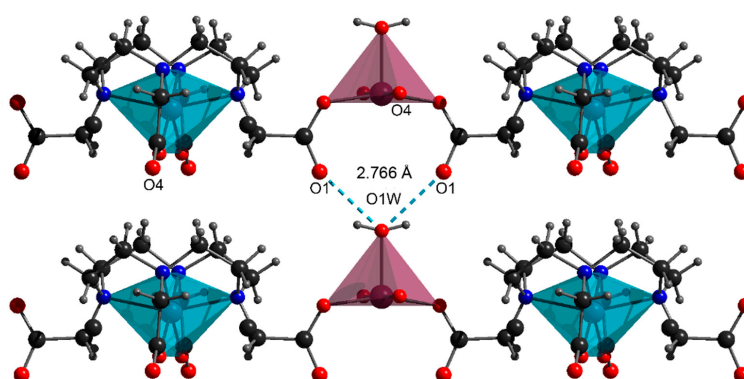


**Figure S4.** X-band EPR spectrum of Cu-DOTA, experimental (blue) and simulated (red). Simulation data:  $g_{xx} = g_{yy} = 2.083$ ,  $g_{zz} = 2.290$ ;  $A_{xx}\{^{63,65}\text{Cu}\} = A_{yy}\{^{63,65}\text{Cu}\} = 20$  G,  $A_{zz}\{^{63,65}\text{Cu}\} = 40$  G.

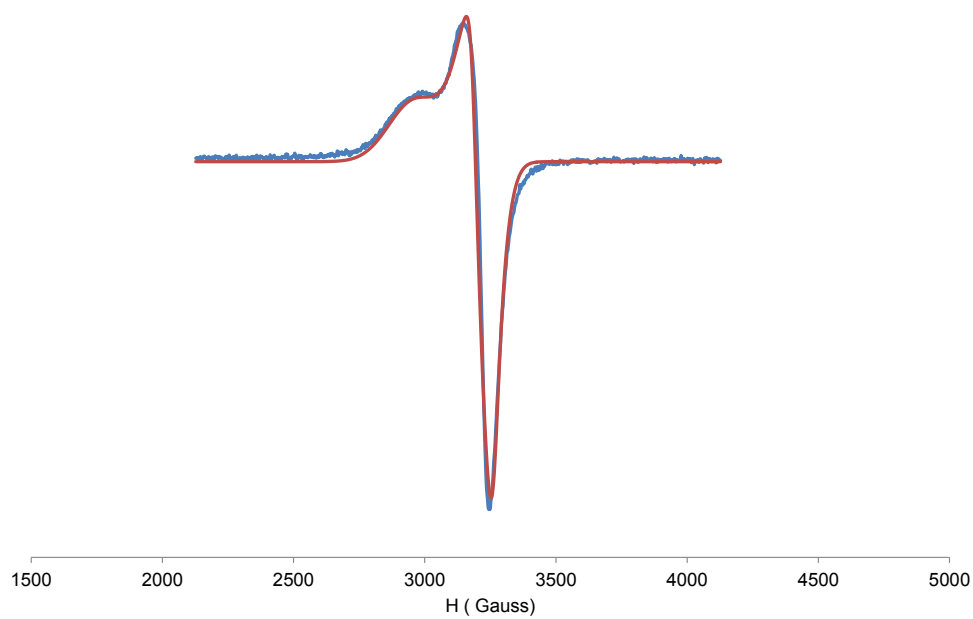


**Figure S5.** X-band EPR spectrum of  $\mathbf{1}_{\text{CuZn}}$ , experimental (blue) and simulated (red). Simulation data:  $g_{xx} = g_{yy} = 2.085$ ,  $g_{zz} = 2.240$ ;  $A_{xx}\{\text{}^{63,65}\text{Cu}\} = A_{yy}\{\text{}^{63,65}\text{Cu}\} = 20$  G,  $A_{zz}\{\text{}^{63,65}\text{Cu}\} = 30$  G.

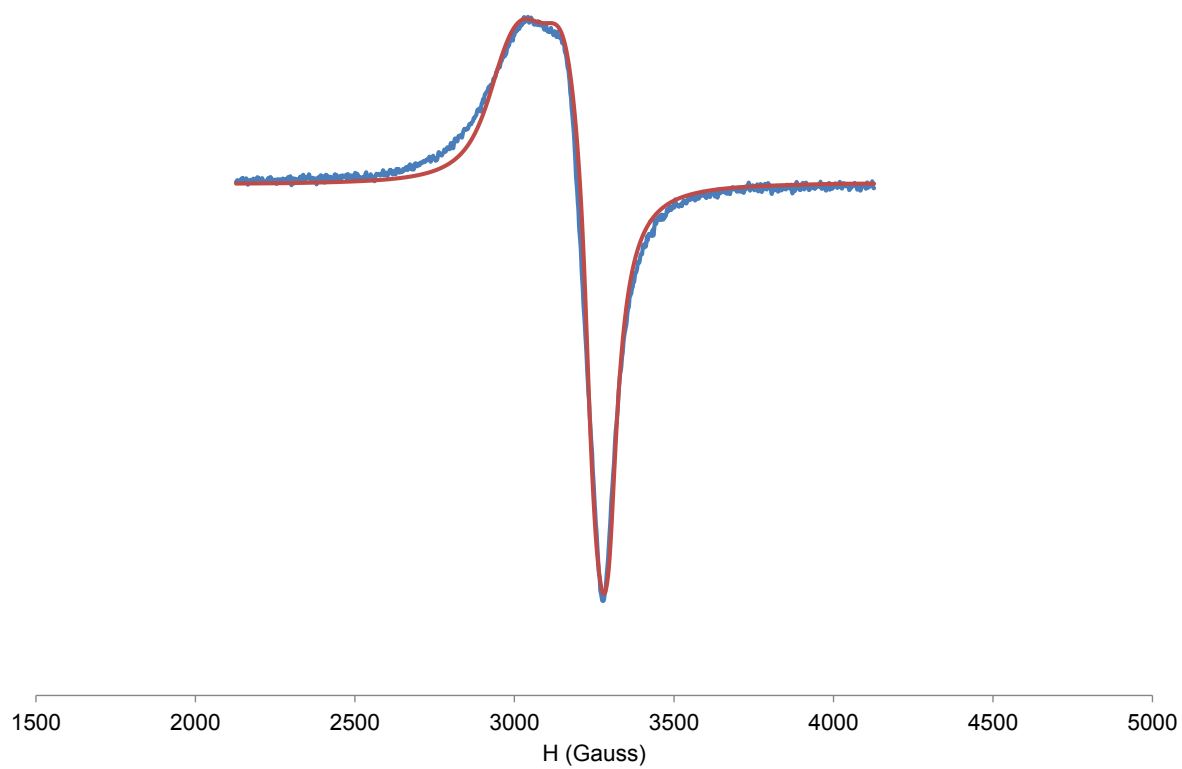


**Figure S6.** Optical microscopy images showing the evolution of the water-triggered transition from  $1_{\text{CuZn}}$  to  $2_{\text{CuZn}}$ .

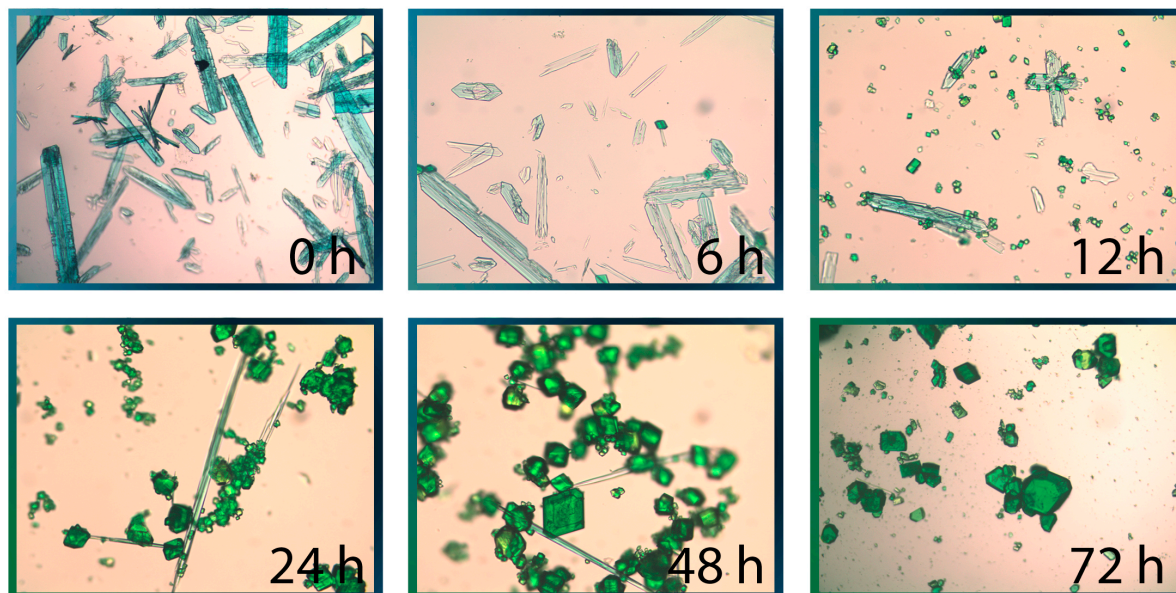


**Figure S7.** XRPD diffractograms of the synthesized  $2_{\text{CuZn}}$  (purple),  $2_{\text{CuCu}}$  (red) and  $2_{\text{CuNi}}$  (blue), as compared to the simulated powder pattern for the crystal structure of  $2_{\text{CuZn}}$  (black).

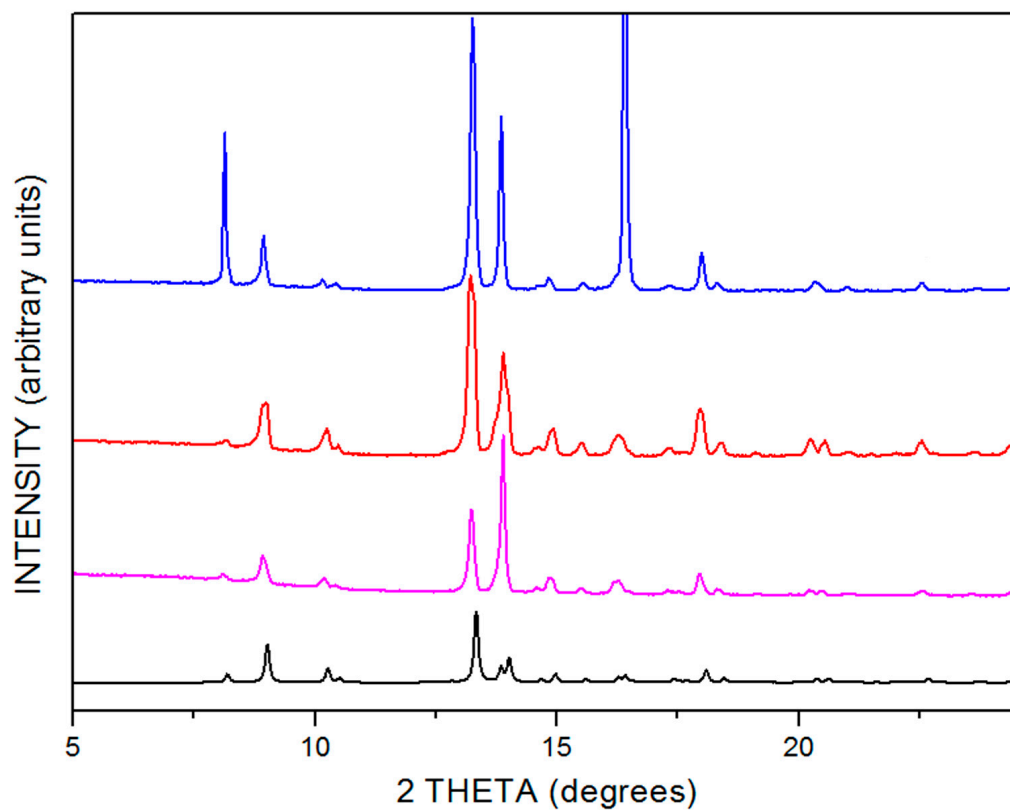


**Figure S8.** Crystal structure of  $2_{\text{CuZn}}$ . (a) Coordination environment on the Cu-DOTA unit and the  $(\text{Zn-Cu})(\text{COO})_4$  hetero-bimetallic paddlewheel unit. (b) View of the ABAB crystal packing across the  $b$  axis, highlighting the interlayer H-bonding water channels (represented as sky-blue dash lines). (c,d) Views of the crystalline lattice across the  $c$  and  $b$  axes, showing the water molecules (represented as red spheres) located in the channels.

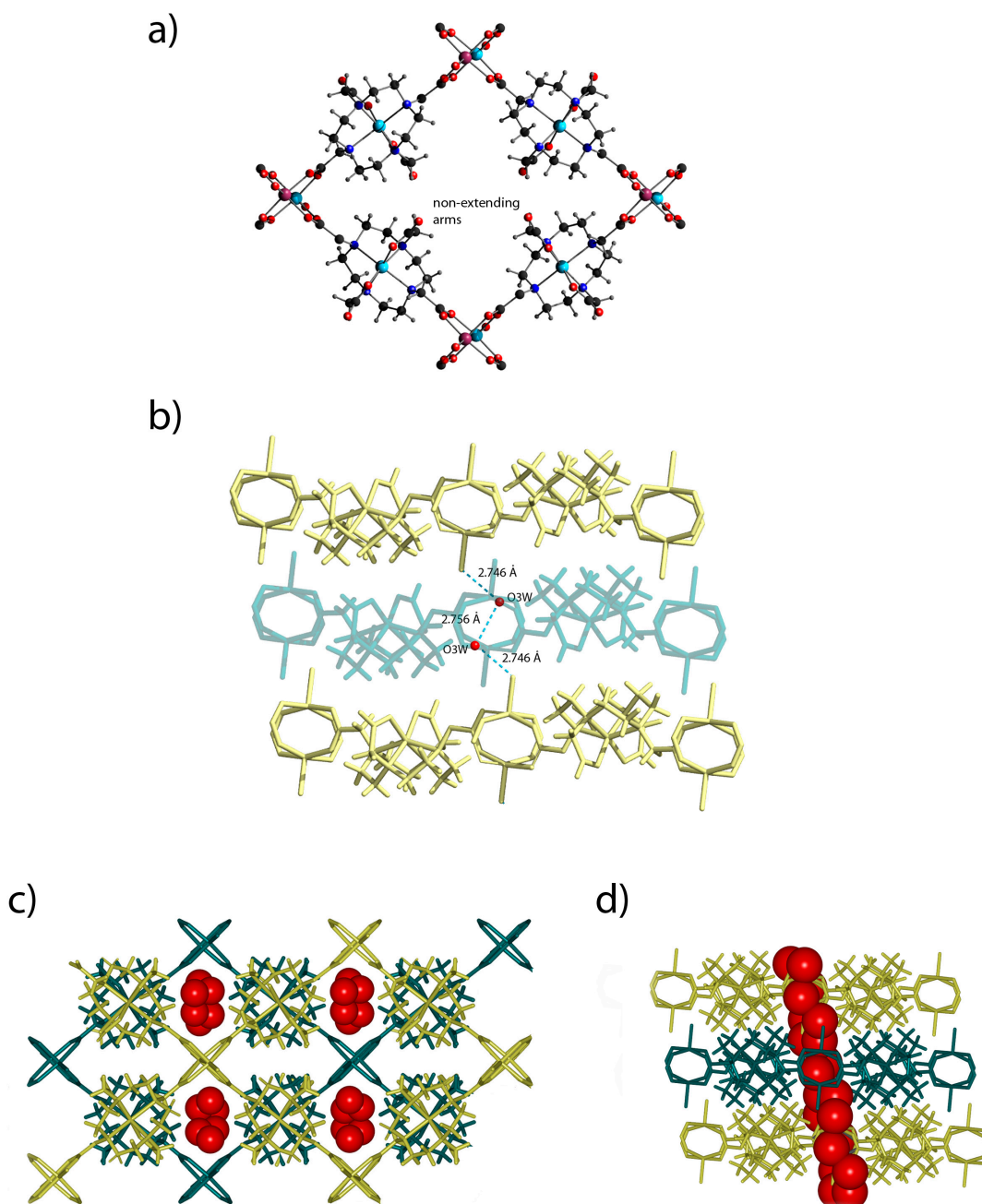


**Figure S9.** XRPD diffractograms of the synthesized  $2_{\text{CuZn}}$  after 6 months immersed in water (green) and after 1 hour immersed in boiling water (red), as compared to the simulated powder pattern for the crystal structure of  $2_{\text{CuZn}}$  (black).

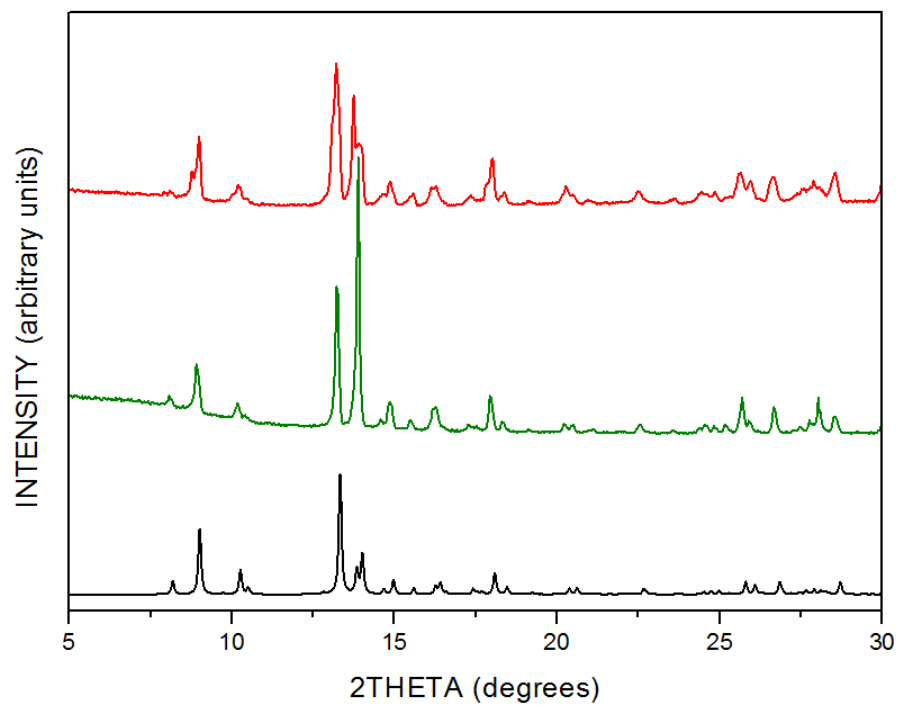


**Figure S10.** Water adsorption isotherm of **1**<sub>CuZn</sub> (blue) and **2**<sub>CuZn</sub> (green).

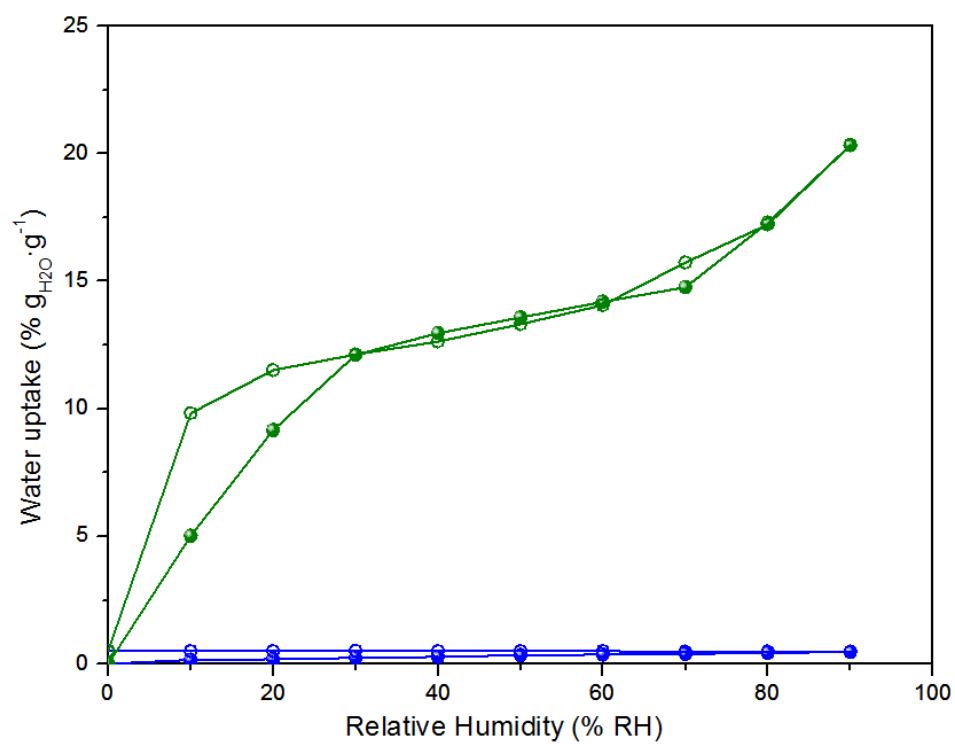


**Figure S11.** XRPD diffractograms of the activated  $2_{\text{CuZn}}$  (blue) and  $2_{\text{CuZn}}$  after measuring the water isotherm (red), as compared to the simulated powder pattern for the crystal structure of  $2_{\text{CuZn}}$  (black).

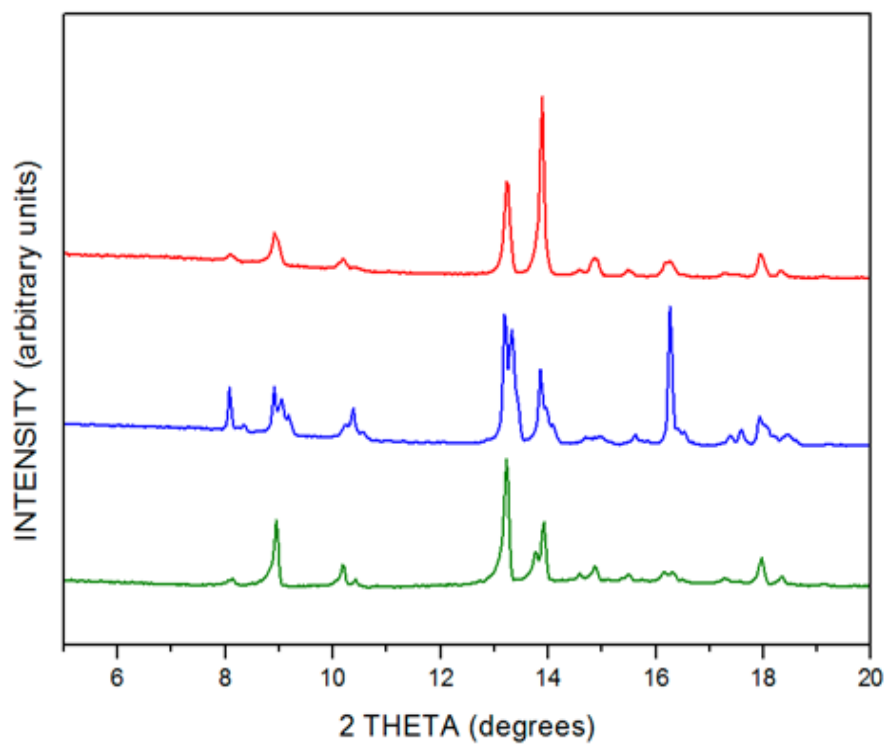
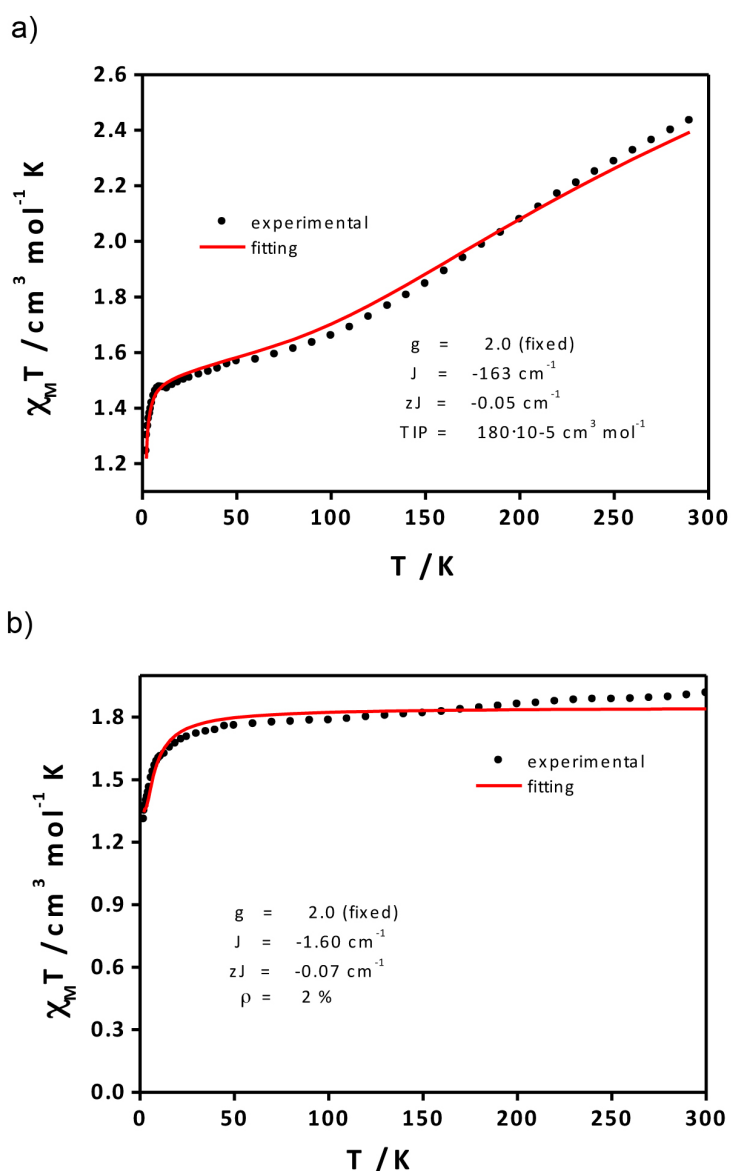


**Figure S12.** Experimental  $\chi_M T$  vs T data of systems (a)  $2_{\text{CuCu}}$  and (b)  $2_{\text{CuZn}}$  (●) and fitting (red line) between 2.0 and 300.0 K using a dc external magnetic field of 1 T. Estimated exchange coupling constant values were achieved by the use of PHI [N. F. Chilton, R. P. Anderson, L. D. Turner, A. Soncini and K. S. Murray *J. Comput. Chem.* **34**, 1164-1175 (2013)] and fixing g (2.0) at all the range of temperatures (2.0 – 300 K) and at the highest (50 K to 300 K) with reasonable fittings. To proceed with, systems were described as one paddle-wheel unit ( $\text{Cu}^{\text{II}}\text{-Cu}^{\text{II}}$  (**1**) and  $\text{Cu}^{\text{II}}\text{-Zn}^{\text{II}}$  (**2**)) surrounded by four mononuclear  $\text{Cu}^{\text{II}}$ -cyclam derivate centers, respectively. In **1**,  $J$  describes the exchange inside the paddle-wheel,  $zJ$  encloses intra/intermolecular interactions among the other centers and TIP has the general meaning. In the case of **2**,  $J$  describes the interaction among the  $\text{Cu}^{\text{II}}$  centre inside the paddle-wheel and the surroundings. It was found that  $J$  values are in a range of  $-160$  to  $-190 \text{ cm}^{-1}$  for **1** and of  $-4$  to  $-2 \text{ cm}^{-1}$  for **2**.



## References

- 1 A. Riesen, M. Zehnder and T. a Kaden, *Helv. Chim. Acta*, 1986, **69**, 2067–2073.